ON THE SIZE SCALING OF CLEAVAGE TOUGHNESS IN THE TRANSITION: A SINGLE VARIABLE EXPERIMENT AND MODEL BASED ANALYSIS

H. J. Rathbun, G. R. Odette and M. Y. He

Department of Mechanical and Environmental Engineering University of California, Santa Barbara
Santa Barbara, CA 93106, USA

ABSTRACT

A systematic investigation of the effects of specimen size on cleavage fracture toughness of a typical pressure vessel steel in the transition is reported. Size dependence of toughness may arise from two basic mechanisms. The first is related to the total volume of material acted on by high stress fields near a blunting crack tip, which is a function of the crack front length (B) in small scale yielding (SSY). We call this the statistical stressed volume (SSV) effect. The second is due to SSY constraint loss (CL), which depends on the ligament length (b) as well as B. Until now, it has not been possible to quantify the individual and combined effects of SSV and CL (or B versus b) size scaling laws, or even to verify fully the existence of the underlying mechanisms. In order to develop a single variable database on size effects, a complete B-b matrix of fracture specimens, fabricated from a single plate of steel from the Shoreham pressure vessel, was tested at a common set of conditions. The B ranged from 8 to 254 mm and b from 3.2 to 25.4 mm. The database was analyzed using 3-dimensional finite element simulations of the crack tip fields, calibrated to the local fracture properties of the Shoreham steel. The finite element based analysis shows that both SSV, giving rise to a $B^{-1/4}$-type scaling, as well as CL, evaluated in terms of in-plane areas within critical stress contours, can sometimes play a significant role in the size scaling of transition toughness. The significance of these results to the recently approved Master Curve standard (ASTM E 1921-97) is discussed briefly.

KEY WORDS: Cleavage toughness, statistical and constraint loss effects, fracture models, Master Curve

INTRODUCTION

There has been significant progress in understanding the mechanisms and mechanics mediating the fracture toughness (K_{Jc}) of steels in the cleavage transition regime that qualitatively rationalizes observations of both large scatter and explicit effects of specimen size and geometry. This understanding is based on: a) the concept of critically stressed regions containing a statistical distribution of cleavage trigger particles local to a blunting crack tip; and b) realistic finite element (FE) simulations of the corresponding stress fields, including 3-D computations, for conditions that deviate substantially from SSY [1,2,3]. Statistical considerations dictate that fracture toughness increases with decreasing volume of material under high stress, giving rise to an inverse power dependence on the crack front length, or thickness, B, in standard edge cracked specimens. We will refer to this as the statistically stressed volume (SSV) effect. Reductions in the crack tip stress amplitude associated with tri-axial constraint loss (CL) can also result in increasing toughness with decreasing specimen dimensions [3] outside the SSY regime. The challenge is to define the limits of SSY, which is complicated by the fact that both SSV and CL effects can appear to have quite similar dimensional scaling in some regimes [4].

Unfortunately, the body of data to quantify the individual and combined contributions of SSV and CL to size effects is rather sparse. A recent review found that the available fracture toughness database is generally inconclusive, since it is dominated by specimens with simultaneous variations in all dimensions, and most

often has ambiguous levels of constraint [5]. Further, the magnitude of CL depends on the detailed micromechanics of cleavage, hence, on the material and microstructure.

These fundamental issues have significant practical implications to the recent ASTM standard master curve (MC) method for measuring K_{Jc} in the transition (ASTM E 1921-97) [6]. The MC method uses an explicit SSV adjustment of $K_{Jc}(B)$ to a common reference B_r = 25.4 mm to account for size effects as $K_{Jcr} = K_{min} + [K_{Jc}(B) - K_{min}][B_r/B]^{1/4}$, where K_{min} = 20 MPa$\sqrt{m}$ is an assumed minimum toughness [1]. A relatively favorable constraint limit is used to 'censor' data affected by CL, and a statistical procedure is used to include the censored data in determining a reference temperature (T_o) at K_{Jc} of 100 MPa$\sqrt{m}$. The maximum toughness limit for uncensored data is determined from a non-dimensional CL factor $M = Eb\sigma_{ys}/K_J^2$ at M = 30, where σ_{ys} is the yield stress, E is the elastic modulus and b is the ligament length[2].

The overall objective of this work is to develop and analyze a single variable database on size effects on K_{Jc} in a typical pressure vessel steel. Specifically, we seek to assess, and physically model, the individual and combined contributions of SSV (B) and CL (b and B) mechanisms.

EXPERIMENTAL: A SINGLE VARIABLE SIZE SCALING STUDY

A full test specimen matrix included variations in B for a set of constant b, and variations in b for a set of constant B. The nominal values of B and b were 8, 16, 32, 64, 127 and 254 mm (B), and 25.4, 12.7, 6.3 and 3.2 mm (b), respectively[3]. A section of ASTM A533 Grade B Class 1 plate from the decommissioned Shoreham vessel was machined into single edge notched three point bend specimens (SENB) in the L-S orientation with span (S) to width ratio S/W=4 and a/W 0.5 . Individual specimen types were taken from randomized locations within the original steel plate. Pre-cracking procedures were developed to ensure straight crack fronts at a constant 1/4 plate thickness depth. Based on preliminary measurements of T_o using 1T C(T) specimens, all quasi-static loading rate tests were carried out at -91°C. With minor or necessary exceptions, including atypical specimen geometry (e.g., large and small B/W ratios), the fracture tests followed the basic ASTM E 1921-97 procedures. For b= 25.4 mm, M is greater than 100 up to 175 MPa$\sqrt{m}$, reasonably assuring negligible to modest CL effects in all but the thinnest specimens. The large range of B from 8 to 254 mm produces a maximum variation of a factor of about 2 in the mean toughness for SSV scaling. The variations in b were used to explore a wide range of constraint conditions, down to M values of less than ten[4]. Eight tests were carried out at each matrix point. Other characterization studies include: a) fracture tests on the 1T C(T), pre-cracked Charpy (PCC) bend bars with a/W of about 0.1 and 0.5, and 1/2 and 1/3-sized PCC bend bars; b) tensile properties at a wide range of temperature; c) metallograpy, micro-hardness and quantitative fractography[5]. Further details on the experimental procedures will be given in future publications.

EXPERIMENTAL RESULTS AND DATABASE

In all cases, fracture was by cleavage initiation with little or no stable crack growth[6]. Figure 1a shows a composite plot of the unadjusted toughness data for various specimens (K_{sp}) plotted against log B (in mm). For clarity, only the maximum and minimum K_{sp}, connected by lines, along with the K_{sp} average for a given B, are shown. The heavy dashed line is a least square fit to the average K_{Jc} data for the largest b = 25.4 mm specimens using the MC form as $K_{min} + [K_{Jc} - K_{min}] [B_r/B]^p$. In this case p = 0.26± 0.09, in almost exact agreement with the nominal SSV prediction. While they are somewhat difficult to see in this very busy plot, three other trends can be observed: a) the minimum K_{sp} is relatively independent of B and b; b) both the average and maximum K_{Jc} generally increase with decreasing B; and c) both the average and maximum K_{Jc} tend to be higher for smaller b. Figure 1b shows the SSV adjusted K_{ssv} averaged for the six B plotted on an

[1] The $B^{-1/4}$ size scaling fundamentally derives from the fact that for SSY, the in-plane area within a specified stress contour varies as the applied K_J^4. Thus, the corresponding volume within a specified stress contour scales with BK_J^4. Assuming a critically stressed volume cleavage criteria gives rise to the $B^{-1/4}$-type scaling.

[2] Other important specimen dimensions are the crack depth (a), width (W) and ligament length (b = W-a).

[3] Due to problems in reliable pre-cracking, the specimens at the matrix point b = 3 mm, B = 64 mm were not tested.

[4] Note, while we have characterized constraint in terms of the in-plane ligament dimension b, loss of out-of-plane (transverse) plane strain constraint also occurs in thin (small B) specimens

[5] The fractography-fracture reconstruction efforts include optical, scanning electron and confocal microscopy. These techniques are being combined to identify fracture initiation sites and process zone damage development sequences.

[6] The maximum stable crack growth in the smallest specimens with the highest toughness was less than 5% of the ligament.

expanded scale against b. Clearly, significant CL effects may occur at nominal values of M_{nom} (also shown, assuming K_{Jc} = 100 MPa m) greater than 30. However, given the large range of specimen geometry in this database, additional analysis of the SSV and CL effects requires application of more detailed size scaling models.

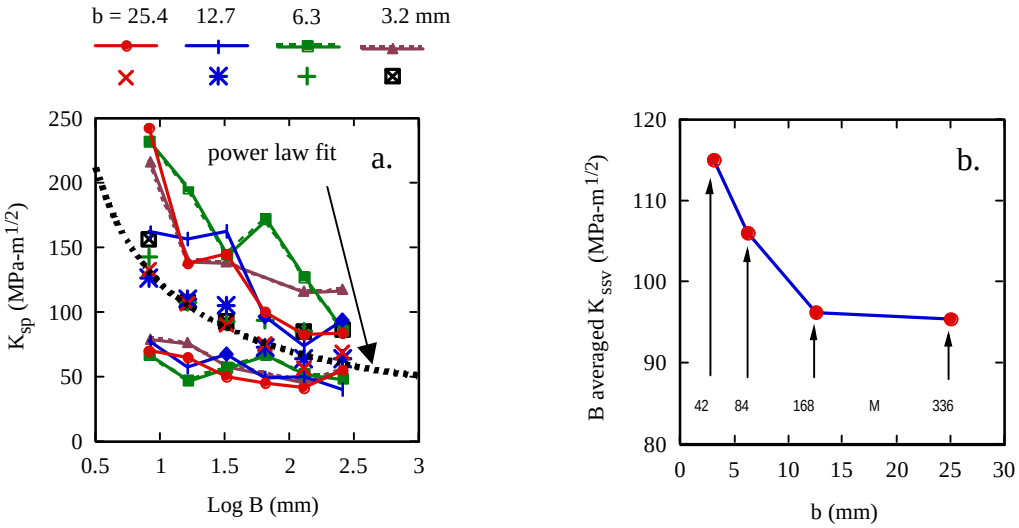

Figure 1 a) Maximum, minimum and average K_{sp} data vs. B; b) K_{ssv} data averaged over B vs. b.

FINITE ELEMENT MODELING OF TOUGHNESS AND SIZE SCALING

Three-dimensional (3-D) finite element (FE) simulations of crack tip stress and strain fields were used to analyze the database described in the previous section, following the general approach of Nevalainen and Dodds [3]. This method assumes that cleavage occurs when a specified principle stress ($\sigma_1 = \sigma^*$) contour encompasses a critical volume (V*) of material in front of the blunting crack tip[7]. Assuming B is fixed, the constraint adjustment is given by the ratio of the applied K_J for a finite specimen (K_{sp}) producing a particular stressed volume (V_{sp}), to the corresponding SSY K_{ssy} that produces the same stressed volume (i.e., $V_{ssy} = V_{sp}$), or K_{sp}/K_{ssy}. However, we also wish to consider variations in B relative to a reference thickness, B_r. Thus, it is most convenient to evaluate V_{sp} as $<A_{sp}>B$, where $<A_{sp}>$ is the stressed area averaged over the entire crack front. The corresponding reference V_{ssy} is $A_{ssy}B_r$, where A_{ssy} is the stressed area for plane strain conditions at a minimal level of global plastic deformation with no T-stress field. The measured toughness can be adjusted to SSY conditions at $B = B_r$, K_{Jcr}, by dividing by the corresponding FE based K_{sp}/K_{Jcr} factor at $<A_{sp}>B = A_{ssy}B_r$. Following Nevalainen and Dodds, the SSY $A_{ssy}(K_J, \sigma_1/\sigma_{ys})$[8] were computed based on an elastic boundary layer analysis using the general purpose FE code ABAQUS [7]. The mesh, consisting of 1200 two dimensional, eight-noded continuum plane strain elements, was very refined near the crack tip, and increased in size out to a large boundary radius. This ensured that the plastic zone was deeply embedded in an elastic zone bounded by imposed elastic displacements with a T-stress equal to 0.

A quarter-symmetry mesh composed of 2480 20-noded quadratic brick elements was used in the 3-D FE simulations for all the non self-similar specimen geometries. Wedge-shaped elements, with overlapping nodes at an initially sharp crack tip, were used to efficiently model blunting up to high levels of gross specimen plastic deformation, corresponding to a minimum M of less than 10. The K_{sp}/K_{Jcr} adjustment accounts for both SSV and CL mediated size-scaling effects[9]. In the SSY regime, $K_{sp}/K_{Jcr} = [B/B_r]^{1/4}$, while the effects of constraint loss can be isolated by assuming $K_{sp}/K_{Jcr} = [A_{ssy}(K_J)/<A_{sp}(K_J)>]^{1/4}$. For a given constitutive law, the CL adjustment depends only on $\sigma_1/\sigma_{ys} = \sigma^*/\sigma_{ys}$.

The A_{ssy} can be represented in a compact non-dimensional form as $A_o = \log[A_{ssy}(\sigma_1/\sigma_{ys})\sigma_{ys}^4/K_J^4]$, and fitted to a polynomial $f(\sigma_1/\sigma_{ys})$ [3]. This relation can be used to evaluate K_{Jc} at specified values of $\sigma_1 = \sigma^*$, $A_{ssy} = A^*$ and σ_{ys}. Further, it has been shown that the predicted $K_{Jc}(T)$ curve shape for unirradiated steels

[7] Statistical variations in trigger particle microstructures result in a corresponding distribution of σ*–V* leading to the inherent scatter of K_{Jc} data in the transition.

[8] The compact nomenclature in this paper uses K_J rather than J, as $K_J = JE'$, where E' is the plane strain modulus.

[9] Note that since the details of the FE computations and analysis procedure were somewhat different for the SSY boundary element and 3-D specimen cases, the A_{ssy}/A_{sp} approaches unity at $M \approx 200$. Thus, no constraint correction is applied for specimens in which the measured $M \geq 200$.

with T_o below 0°C is consistent with the MC shape assuming that σ* and A* are constant (independent of T) using a generic empirical $\sigma_{ys}(T)$ relation [8]. Thus, the model can be used to fit SSY $K_{Jc}(T)$ data to estimate the σ*-A*. The results of fitting are shown in Figure 2a, where the filled circles are data from 1T C(T) specimens and the open diamonds are for PCC specimens SSV adjusted to B_r = 25.4 mm (a/W 0.5 in both cases). Note that this data has not been CL adjusted, which would generally be small. The solid line is the MC shape with T_o = -91°C. The heavy dashed curve is the predicted $K_{Jc}(T)$ curve for A* = 3.7x10^{-8}m^2 and σ* = 1790 MPa - σ^*/σ_{ys}(= 591 MPa) 3. The light dashed lines show the results for fits with a σ^*/σ_{ys} ratios of 2.75 and 3.25. An additional fitting criterion for σ*-A* was that the predicted $K_{Jc}(T)$ match the MC shape in the lower shelf-knee regime (in this case down to –196°C). Thus, the nominal estimate of σ^*/σ_{ys} = 3 is certainly reasonable, but not completely unique. Figure 2b shows a 3-D plot of the effect of B/W and M on CL in terms of the K_{sp}/K_{ssy} for σ^*/σ_{ys} = 3. Additional details regarding the FE simulations and use of alternative statistical models, as well as the insight gained from the other characterization studies, will be presented in future publications.

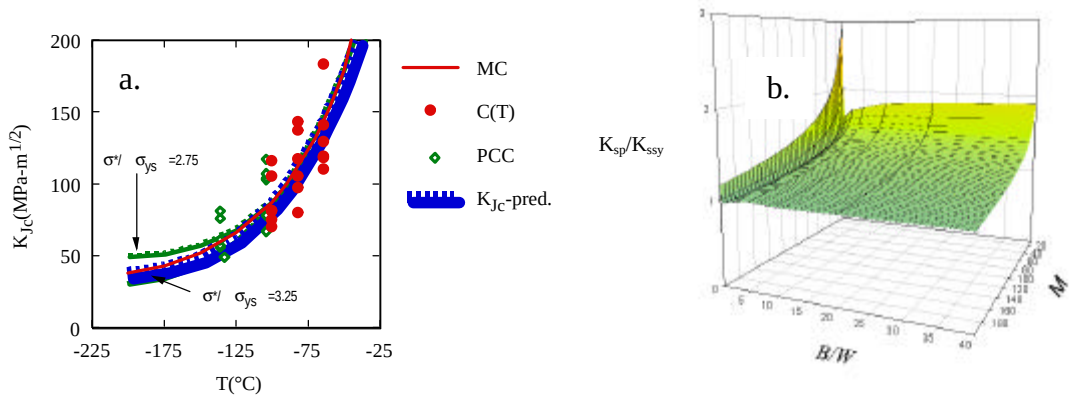

Figure 2 a) The fitted σ*-A* $K_{Jc}(T)$ model; b) FE K_{sp}/K_{ssy} adjustment factor vs. B and M.

ANALYSIS AND EVALUATION OF THE DATABASE

The SSV and CL adjusted K_{Jcr} are shown in Figure 3a plotting the average K_{Jcr} versus B at the 4 ligament (b) lengths. In all cases, the toughness averaged over all B at each b is slightly less than the preliminary estimate of 100 MPa m. The overall average at all B and b is 91.1±4 (at 1 SD) MPa m. The K_{Jcr} average over B for the three largest b are nearly identical at 93±0.2 MPa m, while the corresponding average is only 85.4 MPa m for the smallest b = 3.2 mm. The overall dependence of the average K_{Jcr} on B at various b, as well as on b at various B, is weak and statistically insignificant.

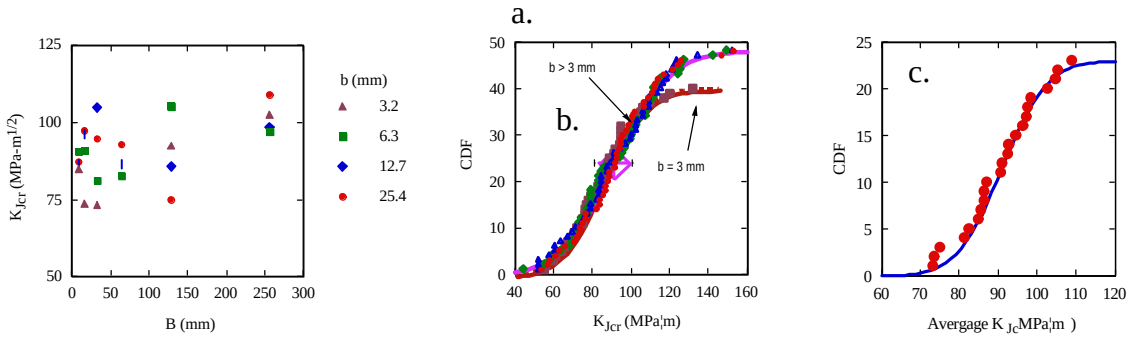

Figure 3 a) Average K_{JCr} for all b-B; b) CDF for the average K_{JCr}; c) CDF for all K_{Jcr}

Figure 3b plots the cumulative distribution of all 180 of the individual adjusted K_{Jcr} data points. The distributions are nearly identical for the three largest b (48 data points each) with a standard deviation (SD) of 23.0±1 MPa m. The corresponding distribution for the 40 data points at the smallest b = 3.2 mm is somewhat narrower and shifted to slightly lower K_{Jcr}. However, in both cases, the data are well represented by a normal cumulative distribution function (CDF), shown by the solid and dashed line for the appropriate average K_{Jcr} and SD. Figure 3c plots a cumulative distribution of the averages at each of the 23 B-b combinations. The standard deviation of this adjusted data set is ±10 MPa m. These data are also

reasonably consistent with a normal CDF, shown by the solid line. The largest deviations are for two of the small b = 3.2 mm specimens with somewhat atypical B/W ratios of about 2.5 and 5. A Monte Carlo simulation, assuming a population of K_{Jcr} data with a SD of 23 MPa m, gave a corresponding SD for the averages for the B-b combinations of 8.1 MPa m, close to the observed value of 10. Figure 4 shows Weibull plots of all the K_{sp}, K_{ssv} and K_{Jcr}, along with corresponding least square (dashed lines). The unadjusted K_{sp} data are for different specimen sizes, hence, are not expected to follow a Weibull distribution. However, to the extent that the SSV and CL adjustments 'work', size-independent Weibull distributions, with a slope approaching m = 4, can be anticipated for K_{ssv} and K_{Jcr}. Thus the low Weibull slope for K_{ssv} of m = 3.17, and deviations at higher toughness, again suggest that the SSV adjustment alone is not sufficient to account for size effects in this dataset. However, the combination of a SSV and CL adjustment results in Weibull slope of m = 3.85 and smaller deviations at high K_{Jcr}. At intermediate K_{Jcr}, the slope is almost exactly equal to the theoretical value of 4.

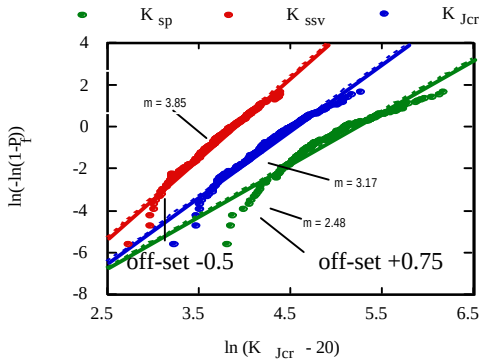

Figure 4 Weibull plots of the K_{sp} (far right), K_{ssv} (middle) and K_{Jcr} (far left) data (offset for clarity).

These results lead to two major conclusions. First, the Shoreham plate is relatively homogeneous at the sampling location with a mean reference toughness of about 92±8 MPa m at –91°C. Second, the combination of the CL and SSV adjustments produce a self-consistent K_{Jcr} data set. Thus, together with this database, the FE model-based adjustments provide a basis to distinguish the *separate and combined* effects of SSV and CL.

Figure 5a shows a decomposition of the adjustments for the various b and B. The unadjusted K_{sp} data point, furthest to the left, is connected to the adjoining K_{ssv} data point to its immediate right. Note, this *accepts* a primary $B^{-1/4}$ scaling adjustment, which reduces K_{ssv} relative to K_{sp} for B < 25.4 mm and has the opposite effect for B > 25.4 mm. The next point to the right reflects the additional CL adjustment that is needed, in some cases, to produce a fully size-independent to K_{Jcr} data set, based on the FE σ*-A* local fracture model. The solid and dashed lines are the average adjusted K_{Jcr} and the ±10 MPa m standard deviation respectively. As expected, the SSV adjustment increases with those B that deviate more from the reference B_r = 25.4 mm, and CL adjustments are most significant at small b and B.

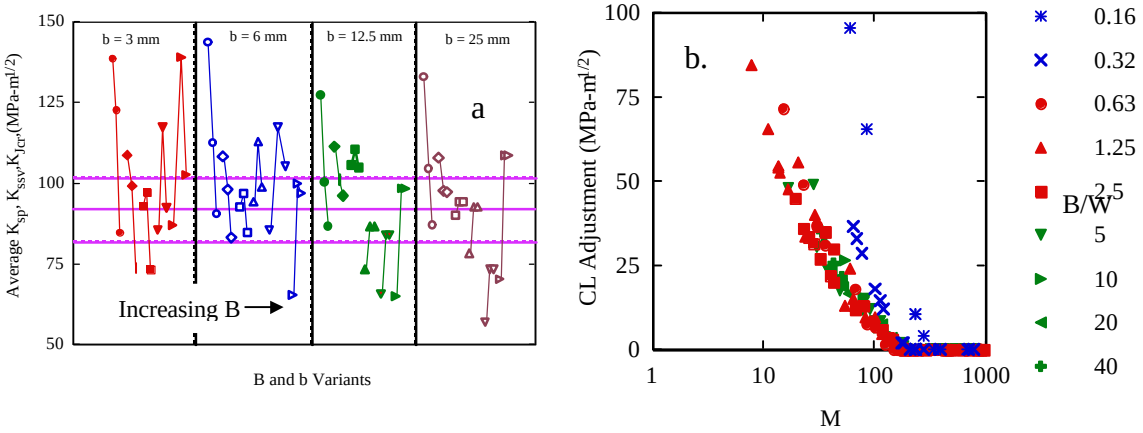

Figure 5 a) The K_{sp}, K_{ssv}, K_{Jcr} adjustment map, with increasing B in going from left to right;
b) the CL adjustment vs. M for various B/W.

Figure 5b plots the CL adjustments (= K_{ssv}-K_{Jcr}) versus M on a log scale (for clarity). The adjustments for the cases with atypically large and small B/W (< 0.5 and > 5) suffer somewhat (high B/W) to significantly (low B/W) larger CL at a given M. The mechanics leading to higher CL with very large B/W

will be discussed in future publications. The data points with B/W ratios from about 0.63 to 2.5, more typical of specimen configurations, are similar. These results suggest that CL begins at M 100 and becomes significant (CL adjustments 10 MPa m) for M from about 50 to 80. Note, a similar analysis using a σ^*/σ_{ys} = 3.25, rather than the nominal value of 3, suggests that CL begins at M slightly less than 100, and becomes significant for an M from about 30 to 50. Further, the M marking significant CL may be lower for compact tension specimens, with a smaller T-stress compared to bend bars.

The individual data sets can also be used to derive T_o, which average -84±9.3°C, and are also reasonably represented by a normal distribution. The highest T_o values are again for the b=3.2 specimen group with B/W = 2.5 and 5. Additional results on the effect of specimen size on the evaluation of T_o will be reported in the future.

SUMMARY AND FUTURE WORK

The results of this study present a remarkably clear picture of size scaling effects on K_{Jc} in the cleavage transition. They demonstrate that SSV *and* CL effects are both significant in some cases. Modeling the combined effects of SSV and CL, using FE simulations of crack tip stress fields, provides a basis for adjusting K_{Jc} data to a common reference size and SSY condition. The database and analysis supports the MC method approach to adjusting toughness data to account for the effect of B. However, the results also indicate that the use of M = 30 may not always fully account for CL.

The results and conclusions reported here should be considered preliminary. As well as additional modeling and statistical evaluations[10], information and physical insight emerging from both the broader characterization and toughness testing efforts will be incorporated in future data analysis. Further, additional testing may be warranted to fill in some gaps and resolve some uncertainties, such as the apparently low values of K_{Jcr} for two B at the smallest b.

ACKNOWLEDGEMENTS

This work was primarily supported by U.S. Nuclear Regulatory Commission Contract NRC-04-94-049. Support was also provided by the U.S. Department of Energy Grant #DE-FG03-87ER-52143 (for much of the FE modeling) and, most recently, the UCSB College of Engineering (for H. Rathbun). We also wish to acknowledge the collaboration of Dr. Robert L. Tregoning for assisting in testing of the largest fracture specimens at the Carderock Division Naval Surface Warfare Center, as well as Tom Huang, David Gragg and Kirk Fields for their help in the fracture testing carried out at UCSB. Finally, we thank Professors Gene Lucas, Robert Dodds and Kim Wallin for helpful discussions and suggestions.

REFERENCES

1. Ritchie, R.O., Knott, J.F., and Rice, J.R. (1973) *J. Mech. Phys. Solids*, 21, 395.
2. Wallin, K. (1991) In: *Defect Assessment in Components - Fundamentals and Applications*, ESIS/EGF9, pp. 415-445, Blauel, J.G. and Schwalbe, K.-H. (Eds.). Mechanical Engineering Publications, London.
3. Nevalainen, M. and Dodds, R.H., Jr. (1995) *Int. Journal of Fracture*, 74, 131.
4. Rathbun, H.J., Odette, G.R., He, M.Y., Lucas, G.E. and Sheckherd, J.W. (1999) In: *Fracture, Fatigue and Weld Residual Stress, PVP-Vol. 393*, pp. 17-22, Pan, J. (Ed.) ASME, New York.
5. Rathbun, H.J., Odette, G.R. and He, M.Y. (2000) In: *Applications of Fracture Mechanics in Failure Assessment, PVP-Vol. 412*, pp. 113-124, Lidbury, D. (Ed.) ASME, New York.
6. ASTM E 1921-97, "Standard Test Method for Determination of Reference Temperature, T_0, for Ferritic Steels in the Transition Range," ASTM 1998.
7. ABAQUS V5.8, ABAQUS Standard Users Manual, Hibbitt, Karlsson and Sorenson, Inc, Providence Rhode Island, 1998.
8. Odette, G.R. and He, M.Y. (2000) *Journal of Nuclear Materials*, 283-287, 120.

[10] Because of length limits in this paper, we have not discussed a number of important issues. These issues include interactions between SSV and CL effects and the trends observed in the lower tail of the K_{Jcr} distribution in relation to the proposal of a threshold toughness of 20 MPa m. These and other topics will be covered in future publications.